



## Well-Balanced Conservative Central Upwind Scheme for Solving the Dam-Break Flow Problem Over Erodible Bed

S. Jelti, A. Serghini and A. El Hajaji

**ABSTRACT:** This work deals with the numerical solution of dam-break flow over an erodible bed. The mathematical model is a combination of the shallow water, the transport diffusion and the bed morphology change equations. The system is solved by a well-Balanced central upwind scheme with conservative property. Several tests are illustrated in order to validate the accuracy and the performance of the model. A comparison of central upwind scheme and Roe scheme is presented.

**Key Words:** Finite volume method, dam-break flow, sediment transport, erodible bed, central upwind scheme.

### Contents

<b>1 Introduction</b>	<b>1</b>
<b>2 The mathematical model</b>	<b>2</b>
2.1 Governing Equations . . . . .	2
2.2 Empirical functions . . . . .	3
<b>3 Numerical scheme</b>	<b>4</b>
3.1 Central-upwind scheme . . . . .	4
3.2 Second order approximation in space . . . . .	5
3.3 Second order approximation in time . . . . .	6
3.4 Discretization of the source term . . . . .	7
<b>4 Numerical results</b>	<b>9</b>
4.1 Verification of the C-property . . . . .	9
4.2 Performance test . . . . .	10
4.3 Dam-break over mobile bed . . . . .	10
4.3.1 Sediments size effect . . . . .	10
4.3.2 Comparison between Roe scheme and Modified central upwind . . . . .	11
<b>5 Conclusion</b>	<b>11</b>

### 1. Introduction

The scientific community continues to search the best possible solutions to develop the numerical modeling of alluvial rivers, both for economic reasons (water reserve, hydropower generation, irrigation, etc. ) and for security reasons (dam-break, flooding prediction, etc.).

The effects of sediment transport and bed changes on the flow have been neglected by the first mathematical models for studying the dam-break flow over movable beds [9,11,18,35]. However, it is obvious that the flow of water play a very significant role in the erosion phenomenon, transport and deposition of sediments; the water flow produces sediment transport and changes in the surface morphology, which in return modify the flow. Therefore, researchers and engineers have been payed attention to the strong interaction between the water flow and the bed morphology change. This concept has given rise to a new mathematical model for a dam-break flow over movable bed [5,7,9], in which they consider two layers simulated separately; the clear water in the upper layer and the mixture of sediment and water in

---

2010 *Mathematics Subject Classification:* 74S10, 65M08, 35K65.

Submitted February 01, 2023. Published April 11, 2023

lower layer. However, the applicability of this model is somehow limited because of the assumption of a constant sediment concentration in the lower layer [10].

*coupled model* has been developed as new mathematical model In [5], which takes into account the strong interaction between flow, sediment transport and morphological evolution of the bed. The coupled model links all conservation equations and provides a synchronous resolution procedure, also, it treats entrainment and deposition sediment as independent processes (this property is called noncapacity model) [6,33].

In this work, we use an unidimensional noncapacity model for a dam-break flow, sediment transport and mobile bed. The mathematical model consists of four equations; the mass and the momentum conservation equation for the water-sediment mixture, the transport diffusion equation for sediment particles and bed morphology change equation, together with empirical formulations for bed friction and sediment exchange between the water column and the bed [33].

Central-upwind schemes were introduced at first in [20,21,22] for one dimensional hyperbolic systems of conservation laws and its multidimensional extensions. The central-upwind schemes belong Godunov central schemes family, therefore they enjoy the main advantages of central schemes for solving time-dependent differential equations in different fields like robustness, simplicity and high-resolution. At the same time, in central upwind a more careful estimate of the one-sided local speeds of propagation and integration over Riemann fans with variable sizes is used (see [24], for instance). This decreases the numerical dissipation and results in increased resolution of the computed solution. Central-upwind schemes have been proposed for general hyperbolic system of conversation law in [24,25] and extended to the shallow water equations and related models in [17,22,23,26].

The governing equations are solved numerically using central upwind scheme. The main goal is to modify the classical central upwind scheme in order to introduce a new formulation to discretize the source term which satisfies the C-property. The MUSCL method with generalized minmod limiter and the Runge-Kutta are used to achieve a second order accuracy.

Particular attention is given to the evolution of the dam-break flow, sediment transport and bed morphological development. Additional test problems are studied in order to validate the proposed scheme. Many previously evolutionary behaviors of dam-break over erodible bed are addressed in [7], [10], [6] and [15] and many unreported features are interpreted, such as the effect of the sediment size on the free surface and bed mobility profiles. The result expected from this work is to warrant a satisfying accuracy and synchronous solution by coupling all equations. Same works exist with many differences including the numerical method of resolution, [6], [15], [19], [36] and [34].

This work is organized as follows. Section 2 presents the governing equations for a dam-break over erodible sediment bed, as well as the empirical functions considered. In Section 3 the central upwind scheme is introduced and its discretization is given. The treatment of the source term is introduced in Section 3.4. Section 4 covers the tests and the numerical results. Finally a conclusion is given in Section 5.

## 2. The mathematical model

In this section, we define the mathematical model and the empirical functions used in this paper. There are many mathematical models developed in the literature, in our study we will use the one presented in [6] which has been used in some recent works like [2], [13], [15] and [30].

### 2.1. Governing Equations

In this step of study, attention is focused on one-dimensional flow in a channel with rectangular cross section of constant width, over a mobile bed composed of uniform and noncohesive sediment particles. This mathematical model can be extendable to natural rivers with complex geometries, nonuniform sediments and multidimensional problems.

The mass and momentum conservation equations for the water-sediment mixture, the mass conservation equation for the sediment and the mass conservation equation for the bed material are written as

[2,6,15,30,33] :

$$\frac{\partial h}{\partial t} + \frac{\partial(hu)}{\partial x} = \frac{E - D}{1 - p} \quad (2.1)$$

$$\frac{\partial(hu)}{\partial t} + \frac{\partial(hu^2 + \frac{1}{2}gh^2)}{\partial x} = B \quad (2.2)$$

$$\frac{\partial(hc)}{\partial t} + \frac{\partial(huc)}{\partial x} = E - D \quad (2.3)$$

$$\frac{\partial z}{\partial t} = -\frac{E - D}{1 - p} \quad (2.4)$$

where  $B$  is the source term defined by :

$$B = -gh \frac{\partial z}{\partial x} - \frac{\rho_s - \rho_w}{2\rho} gh^2 \frac{\partial c}{\partial x} - ghS_f - \frac{\rho_0 - \rho}{\rho} \frac{E - D}{1 - p} u \quad (2.5)$$

$t$  is the time,  $x$  the streamwise coordinate,  $h$  the flow depth,  $u$  the depth-averaged streamwise velocity,  $z$  the bed elevation,  $c$  the flux-averaged volumetric sediment concentration,  $g$  the gravitational acceleration,  $p$  the bed sediment porosity.  $D$  and  $E$  are the sediment deposition and entrainment fluxes across the bottom boundary of flow, they represent the exchange between water column and bed.  $S_f$  is the friction slope,  $\rho = \rho_w(1 - c) + \rho_s c$  is the density of water-sediment mixture,  $\rho_0 = \rho_w p + \rho_s(1 - p)$  is the density of the saturated bed,  $\rho_w$  and  $\rho_s$  are the densities of water and sediment, respectively.

Equation (2.1) represents the mass conservation equation for the water-sediment mixture. It differs from the conservation equation for clear water flows because of the right hand side term, which constitutes the link between sediment, water and bed exchange [6,30]. Equation (2.2) represents the momentum conservation equation for the water-sediment mixture. There are two additional terms on the right hand side comparing with the momentum equation for clear water flows. The first one represents the momentum transfer due to sediment exchange between the water column and the erodible bed boundary. The second one indicates the effect of streamwise variable concentration. The mass conservation equation for sediment is represented by Equation (2.3), in which suspended and bed load are considered in a single mode indicated by the total sediment load. Equation (2.4) indicates the bed change rate.

## 2.2. Empirical functions

To complete the governing equations given above, formulations have to be chosen to determine the friction slope and the sediment entrainment-deposition fluxes across the bottom boundary of the flow. The conventional relation is used to determine the friction slope:

$$S_f = \frac{n_f^2 u |u|}{h^{\frac{4}{3}}} \quad (2.6)$$

which involves the Manning roughness  $n_f = 0.03$ .

In alluvial rivers, sediment exchange between the flow and the erodible bed involves two distinct mechanisms, bed sediment entrainment due to turbulence and sediment deposition due to gravitational action. These two mechanisms are dependant to the problem studied, entrainment in extreme events such as dam-break problems can be more significant than simple fluvial processes, and responsible of bed morphological change. There exists a variety of empirical formulations derived on various cases, we follow those used in [2,4,6,30,33].

For deposition  $D$ , the relation used is:

$$D = \omega(1 - c_a)^m c_a \quad (2.7)$$

$m$  is an exponent set to  $m = 2$ .  $c_a$  is the local near-bed sediment concentration in volume, it is presumed to be proportional to the depth-averaged concentration i.e.,  $c_a = \alpha c$ , where  $\alpha$  is an empirical coefficient usually larger than unity [33]:

$$\alpha = \min \left( 2, \frac{1 - p}{c} \right)$$

$\omega$  is the settling velocity of sediment particle in tranquil water [32,33]:

$$\omega = 1.1 \sqrt{\left(\frac{\rho_s}{\rho} - 1\right) g d}$$

where  $d$  is the diameter of the sediment grain. In our case  $d$  is larger than  $1mm$ .

For the entrainment, we use:

$$E = \begin{cases} \varphi \frac{\theta - \theta_c}{h} \frac{u}{d^{0.2}} & \text{if } \theta \geq \theta_c \\ 0 & \text{otherwise} \end{cases} \quad (2.8)$$

where  $\varphi = 0.015 m^{1.2}$  is a coefficient to control erosion force,  $\theta_c = 0.045$  is the critical value of Shield's parameter for the initiation of sediment motion and  $\theta$  is the Shield's coefficient defined by [6,30]:

$$\theta = \frac{u_*^2}{gd \sqrt{\frac{\rho_s}{\rho_w} - 1}}$$

$u_*$  is the friction velocity defined by :

$$u_*^2 = \sqrt{\frac{f}{8}} \cdot |u|$$

where  $f$  is the Darcy-Weisbach friction factor defined by [30] as

$$f = \frac{8 g n_f^2}{h^{1/3}}$$

### 3. Numerical scheme

Equations (2.1-2.4) constitute a hyperbolic system, which is solved numerically using central-upwind scheme [29]. In this study, Equation (2.4) is coupled to all other equations, this makes the resolution more realistic, but the hyperbolicity of the system becomes more strong [6].

#### 3.1. Central-upwind scheme

It is well known that Godunov-type central schemes are Riemann-problem-solver-free and are robust, simple and high-resolution methods for solving time-dependent differential equations in different fields. The central-upwind schemes belong to Godunov central schemes family, where a more careful estimate of the one-sided local speeds of propagation and integration over Riemann fans with variable sizes is used. This decreases the numerical dissipation and results in increased resolution of the computed solution. Another advantage of these schemes, as opposed to the earlier developed staggered central schemes, is that they can be used for steady state computations. Central-upwind schemes have been proposed for general hyperbolic system of conservation law in [24,25] and extended to the shallow water equations and related models in [22,23,26].

Equations (2.1-2.4) can be arranged in the conservative form:

$$\frac{\partial U}{\partial t} + \frac{\partial F(U)}{\partial x} = S + Q \quad (3.1)$$

or non-conservative form:

$$\frac{\partial U}{\partial t} + A(U) \frac{\partial U}{\partial x} = Q \quad (3.2)$$

where

$$U = \begin{pmatrix} h \\ hu \\ hc \\ z \end{pmatrix}, \quad F = \begin{pmatrix} hu \\ hu^2 + \frac{1}{2}gh^2 \\ huc \\ 0 \end{pmatrix}, \quad S = \begin{pmatrix} 0 \\ -gh \frac{\partial z}{\partial x} - \frac{(\rho_s - \rho_w)}{2\rho} gh^2 \frac{\partial c}{\partial x} \\ 0 \\ 0 \end{pmatrix},$$

$$Q = \begin{pmatrix} \frac{E-D}{1-p} \\ -ghS_f - \frac{\rho_0 - \rho}{\rho} \frac{E-D}{1-p} u \\ E - D \\ -\frac{E-D}{1-p} \end{pmatrix}$$

the matrix  $\mathcal{A}(U)$  is given by

$$\mathcal{A}(U) = \begin{bmatrix} 0 & 1 & 0 & 0 \\ gh - u^2 - \frac{\rho_s - \rho_w}{2\rho} ghc & 2u & \frac{\rho_s - \rho_w}{2\rho} gh & gh \\ -uc & c & u & 0 \\ 0 & 0 & 0 & 0 \end{bmatrix}$$

$\mathcal{A}(U)$  has the four following distinct real eigenvalues

$$\lambda_1 = 0, \quad \lambda_2 = u, \quad \lambda_3 = u - \sqrt{gh}, \quad \text{and } \lambda_4 = u + \sqrt{gh}$$

The spatial domain is discretized into finite volume cells  $\mathcal{C}_i = [x_{i-\frac{1}{2}}, x_{i+\frac{1}{2}}]$  with the same length  $\Delta x$ . The time interval is divided into subintervals  $[t_n, t_{n+1}]$  with uniform size  $\Delta t$ . We suppose that at certain time  $t$ , the solution is given in terms of its cell averages  $U_i = \frac{1}{\Delta x} \int_{\mathcal{C}_i} U(x, t) dx$ , which are given in time according to the semi-discrete central-upwind scheme, see for instance [21,22] as follows

$$\frac{\partial U_i}{\partial t} = -\frac{H_{i+\frac{1}{2}}(t) - H_{i-\frac{1}{2}}(t)}{\Delta x} + S_i(t) + Q_i(t), \quad (3.3)$$

where  $S_i(t)$  and  $Q_i(t)$  are respectively the cell average of  $S(t)$  and  $Q(t)$  on  $\mathcal{C}_i$  at the time  $t$ . The central-upwind numerical flux  $H_{i+\frac{1}{2}}(t)$  are given by

$$H_{i+\frac{1}{2}}(t) = \frac{a_{i+\frac{1}{2}}^+ F_{i+\frac{1}{2}}^-(t) - a_{i+\frac{1}{2}}^- F_{i+\frac{1}{2}}^+(t)}{a_{i+\frac{1}{2}}^+ - a_{i+\frac{1}{2}}^-} + \frac{a_{i+\frac{1}{2}}^+ a_{i+\frac{1}{2}}^-}{a_{i+\frac{1}{2}}^+ - a_{i+\frac{1}{2}}^-} (U_{i+\frac{1}{2}}^+(t) - U_{i+\frac{1}{2}}^-(t)). \quad (3.4)$$

due to the hyperbolicity of the system of differential equations (3.2), the discontinuities appearing at the reconstruction step at the interface points  $x_{i+1/2}$  propagate at finite speeds estimated by

$$a_{i+\frac{1}{2}}^+ = \max \left( 0, u_{i+\frac{1}{2}}^+ + \sqrt{gh_{i+\frac{1}{2}}^+}, u_{i+\frac{1}{2}}^- + \sqrt{gh_{i+\frac{1}{2}}^-} \right) \quad (3.5)$$

$$a_{i+\frac{1}{2}}^- = \min \left( 0, u_{i+\frac{1}{2}}^+ - \sqrt{gh_{i+\frac{1}{2}}^+}, u_{i+\frac{1}{2}}^- - \sqrt{gh_{i+\frac{1}{2}}^-} \right) \quad (3.6)$$

### 3.2. Second order approximation in space

When  $U_{i+\frac{1}{2}}^-$  and  $U_{i+\frac{1}{2}}^+$  are approximated by  $U_i$  and  $U_{i+1}$  respectively, the semi-discrete central-upwind scheme is only first-order accurate in space. However, if we take them as the right and the left point values of the piecewise linear reconstruction on the cell  $\mathcal{C}_i$ , the scheme is second order in space. In our study, we adopt the linear reconstruction given by [8] and then for each  $i$  we put

$$\bar{U}_i(x) = U_i + \left( \frac{\partial U}{\partial x} \right)_i (x - x_i), \quad \forall x \in [x_{i-\frac{1}{2}}, x_{i+\frac{1}{2}}]$$

$U_{i+\frac{1}{2}}^+$  and  $U_{i+\frac{1}{2}}^-$  are the right and left point values of the piecewise linear reconstruction at  $x = x_{i+\frac{1}{2}}$ , then

$$U_{i+\frac{1}{2}}^+ = U_i + \frac{\Delta x}{2} \left( \frac{\partial U}{\partial x} \right)_i \quad (3.7)$$

$$U_{i+\frac{1}{2}}^- = U_{i+1} - \frac{\Delta x}{2} \left( \frac{\partial U}{\partial x} \right)_{i+1} \quad (3.8)$$

The numerical derivatives  $(U_x)_i$  are to be computed using a nonlinear limiter. In this paper the generalized minmod limiter in order to warrant the second order accuracy and a non-oscillatory nature of the reconstruction is used :

$$\left(\frac{\partial U}{\partial x}\right)_i = \text{minmod}\left(\theta\frac{U_{i+1}-U_i}{\Delta x}; \theta\frac{U_i-U_{i-1}}{\Delta x}; \frac{U_{i+1}-U_{i-1}}{2\Delta x}\right)$$

where the minmod function is defined by:

$$\text{minmod}(\alpha_1, \alpha_2, \alpha_3) = \begin{cases} \min(\alpha_1, \alpha_2, \alpha_3) & \text{if } \alpha_i > 0, \forall i \\ \max(\alpha_1, \alpha_2, \alpha_3) & \text{if } \alpha_i < 0, \forall i \\ 0 & \text{otherwise} \end{cases} \quad (3.9)$$

The central-upwind framework allows one to decrease a relatively large amount of numerical dissipation present at the staggered central schemes. In [23], the authors present a modification of the one-dimensional semi-discrete central-upwind scheme, in which the numerical dissipation is more reduced. In this case the central-upwind numerical flux  $H_{i+\frac{1}{2}}(t)$  is given by

$$H_{i+\frac{1}{2}}(t) = \frac{a_{i+\frac{1}{2}}^+ F_{i+\frac{1}{2}}^-(t) - a_{i+\frac{1}{2}}^- F_{i+\frac{1}{2}}^+(t)}{a_{i+\frac{1}{2}}^+ - a_{i+\frac{1}{2}}^-} + \frac{a_{i+\frac{1}{2}}^+ a_{i+\frac{1}{2}}^-}{a_{i+\frac{1}{2}}^+ - a_{i+\frac{1}{2}}^-} (U_{i+\frac{1}{2}}^+(t) - U_{i+\frac{1}{2}}^-(t)) - \mathbf{d}_{i+\frac{1}{2}}, \quad (3.10)$$

where  $\mathbf{d}_{i+\frac{1}{2}}$  is called the correction term or built-in anti-diffusion term and is defined by

$$\mathbf{d}_{i+\frac{1}{2}} = \frac{a_{i+\frac{1}{2}}^+ a_{i+\frac{1}{2}}^-}{a_{i+\frac{1}{2}}^+ - a_{i+\frac{1}{2}}^-} \text{minmod}\left(U_{i+\frac{1}{2}}^+(t) - U_{i+\frac{1}{2}}^*(t), U_{i+\frac{1}{2}}^*(t) - U_{i+\frac{1}{2}}^-(t)\right). \quad (3.11)$$

The intermediate value  $U_{i+\frac{1}{2}}^*(t)$  is given by

$$U_{i+\frac{1}{2}}^*(t) = \frac{a_{i+\frac{1}{2}}^+ U_{i+\frac{1}{2}}^+(t) - a_{i+\frac{1}{2}}^- U_{i+\frac{1}{2}}^-(t) - (F_{i+\frac{1}{2}}^+(t) - F_{i+\frac{1}{2}}^-(t))}{a_{i+\frac{1}{2}}^+ - a_{i+\frac{1}{2}}^-}. \quad (3.12)$$

Consider the modified correction term defined as

$$\mathbf{D}_{i+\frac{1}{2}} = \begin{bmatrix} 2 & 0 & 0 & 0 \\ 0 & 1 & 0 & 0 \\ 0 & 0 & 1 & 0 \\ 0 & 0 & 0 & 2 \end{bmatrix} \cdot \mathbf{d}_{i+\frac{1}{2}} \quad (3.13)$$

and the modified central-upwind numerical flux  $H_{i+\frac{1}{2}}(t)$  given by

$$H_{i+\frac{1}{2}}(t) = \frac{a_{i+\frac{1}{2}}^+ F_{i+\frac{1}{2}}^-(t) - a_{i+\frac{1}{2}}^- F_{i+\frac{1}{2}}^+(t)}{a_{i+\frac{1}{2}}^+ - a_{i+\frac{1}{2}}^-} + \frac{a_{i+\frac{1}{2}}^+ a_{i+\frac{1}{2}}^-}{a_{i+\frac{1}{2}}^+ - a_{i+\frac{1}{2}}^-} (U_{i+\frac{1}{2}}^+(t) - U_{i+\frac{1}{2}}^-(t)) - \mathbf{D}_{i+\frac{1}{2}}. \quad (3.14)$$

The goal of the modified correction term is to obtain a scheme satisfying the Conservation property. This modification is obtained by multiplying the correction term corresponding to  $h$  and  $z$  by 2 and conserve the one corresponding to  $hu$  and  $hc$ .

### 3.3. Second order approximation in time

To reach second order approximation in time, we rewrite relation (3.3) as:

$$\frac{\partial U_i}{\partial t} = \mathcal{L}(U_i) \quad (3.15)$$

then we use the Runge-Kutta second order scheme [12,27]:

$$\begin{cases} U^* = U^n + \Delta t \mathcal{L}(U^n) \\ U^{**} = U^* + \Delta t \mathcal{L}(U^*) \\ U^{n+1} = \frac{1}{2}(U^n + U^{**}) \end{cases}$$

### 3.4. Discretization of the source term

The source term has a great effect on the resolution of the system. For this, we must work out a discretization which satisfy a conservation property, knowing that a simple central discretization of the source term does not hold this property and spurious numerical waves can appear. A scheme verifies the C-property if the initial equilibrium is preserved when  $u^n = 0$ , for each  $n$ , i.e.,

$$E - D = 0, \quad u_i^n = 0, \quad h_i^n + z_i^n = C_1, \quad \rho_i^n = C_2, \quad z_i^n = z(x), \quad \forall n$$

$C_1$  and  $C_2$  are constants. Consequently, the system (3.1) is reduced to

$$\frac{\partial U}{\partial t} + \frac{\partial F}{\partial x} = S \quad (3.16)$$

where

$$U = \begin{pmatrix} h \\ 0 \\ z \end{pmatrix}, \quad F = \begin{pmatrix} 0 \\ \frac{1}{2}gh^2 \\ 0 \end{pmatrix}, \quad S = \begin{pmatrix} 0 \\ -gh\frac{\partial z}{\partial x} \\ 0 \end{pmatrix}.$$

Note that the third equation in (3.1) is automatically satisfied at the equilibrium. The eigenvalues of the system (3.16) are  $-\sqrt{gh}$ ,  $\sqrt{gh}$  and 0 and then, using (3.5) and (3.6), the values of  $a_{i+\frac{1}{2}}^+$  and  $a_{i+\frac{1}{2}}^-$  satisfy the following relation

$$a_{i+\frac{1}{2}}^+ = -a_{i+\frac{1}{2}}^- = \sigma. \quad (3.17)$$

Using (3.12), we obtain

$$U_{i+\frac{1}{2}}^{*,n} = \frac{1}{2}(U_{i+\frac{1}{2}}^{+,n} + U_{i+\frac{1}{2}}^{-,n}) - \frac{1}{2\sigma}(F_{i+\frac{1}{2}}^{+,n} - F_{i+\frac{1}{2}}^{-,n}),$$

then

$$U_{i+\frac{1}{2}}^{*,n} = \frac{1}{2} \begin{pmatrix} h_{i+\frac{1}{2}}^{+,n} + h_{i+\frac{1}{2}}^{-,n} \\ \frac{1}{2\sigma}g(h_{i+\frac{1}{2}}^{+,n})^2 - \frac{1}{2\sigma}g(h_{i+\frac{1}{2}}^{-,n})^2 \\ z_{i+\frac{1}{2}}^{+,n} + z_{i+\frac{1}{2}}^{-,n} \end{pmatrix}.$$

Therefore, from (3.11), we have

$$\begin{aligned} \mathbf{d}_{i+\frac{1}{2}} &= \frac{\sigma}{4} \minmod \left( \begin{pmatrix} h_{i+\frac{1}{2}}^{+,n} - h_{i+\frac{1}{2}}^{-,n} \\ -\frac{1}{2\sigma}g(h_{i+\frac{1}{2}}^{+,n})^2 + \frac{1}{2\sigma}g(h_{i+\frac{1}{2}}^{-,n})^2 \\ z_{i+\frac{1}{2}}^{+,n} - z_{i+\frac{1}{2}}^{-,n} \end{pmatrix}, \begin{pmatrix} h_{i+\frac{1}{2}}^{+,n} - h_{i+\frac{1}{2}}^{-,n} \\ \frac{1}{2\sigma}g(h_{i+\frac{1}{2}}^{+,n})^2 - \frac{1}{2\sigma}g(h_{i+\frac{1}{2}}^{-,n})^2 \\ z_{i+\frac{1}{2}}^{+,n} - z_{i+\frac{1}{2}}^{-,n} \end{pmatrix} \right) \\ &= \frac{\sigma}{4} \begin{pmatrix} h_{i+\frac{1}{2}}^{+,n} - h_{i+\frac{1}{2}}^{-,n} \\ 0 \\ z_{i+\frac{1}{2}}^{+,n} - z_{i+\frac{1}{2}}^{-,n} \end{pmatrix}. \end{aligned}$$

The modified correction term becomes

$$\mathbf{D}_{i+\frac{1}{2}} = \frac{\sigma}{2} \begin{pmatrix} h_{i+\frac{1}{2}}^{+,n} - h_{i+\frac{1}{2}}^{-,n} \\ 0 \\ z_{i+\frac{1}{2}}^{+,n} - z_{i+\frac{1}{2}}^{-,n} \end{pmatrix} = \frac{\sigma}{2}(U_{i+\frac{1}{2}}^{+,n} - U_{i+\frac{1}{2}}^{-,n})$$

and the modified flux defined by (3.14) is given as follows

$$\begin{aligned} H_{i+\frac{1}{2}}^n &= \frac{F_{i+\frac{1}{2}}^{+,n} - F_{i+\frac{1}{2}}^{-,n}}{2} + \frac{\sigma}{2}(U_{i+\frac{1}{2}}^{+,n} - U_{i+\frac{1}{2}}^{-,n}) - \mathbf{D}_{i+\frac{1}{2}} \\ &= \begin{pmatrix} 0 \\ \frac{1}{4}g(h_{i+\frac{1}{2}}^{+,n})^2 - \frac{1}{4}g(h_{i+\frac{1}{2}}^{-,n})^2 \\ 0 \end{pmatrix}. \end{aligned}$$

Using the steady state assumption, we can write

$$U_i^{n+1} = U_i^n$$

From Equation 3.3, we get

$$\frac{H_{i+\frac{1}{2}}^n - H_{i-\frac{1}{2}}^n}{\Delta x} = S_i(t),$$

and then

$$\frac{1}{4}g \begin{pmatrix} 0 \\ (h_{i+\frac{1}{2}}^{+,n})^2 + (h_{i+\frac{1}{2}}^{-,n})^2 - (h_{i-\frac{1}{2}}^{+,n})^2 - (h_{i-\frac{1}{2}}^{-,n})^2 \\ 0 \end{pmatrix} = \Delta x \begin{pmatrix} 0 \\ -g \left( h \frac{\partial z}{\partial x} \right)_i \\ 0 \end{pmatrix}$$

We can rearrange the second member as:

$$\frac{1}{4} \left( h_{i+\frac{1}{2}}^{+,n} - h_{i-\frac{1}{2}}^{+,n} \right) \left( h_{i+\frac{1}{2}}^{+,n} + h_{i-\frac{1}{2}}^{+,n} \right) + \frac{1}{4} \left( h_{i+\frac{1}{2}}^{-,n} - h_{i-\frac{1}{2}}^{-,n} \right) \left( h_{i+\frac{1}{2}}^{-,n} + h_{i-\frac{1}{2}}^{-,n} \right) = -\Delta x \left( h \frac{\partial z}{\partial x} \right)_i \quad (3.18)$$

Knowing that for stationary solution  $h + z = \text{constant}$ , we obtain

$$h_{i+\frac{1}{2}} + z_{i+\frac{1}{2}} = h_{i-\frac{1}{2}} + z_{i-\frac{1}{2}}$$

so, Equation (3.18) becomes

$$\frac{1}{2} \left[ \frac{(z_{i+\frac{1}{2}}^{+,n} - z_{i-\frac{1}{2}}^{+,n})}{\Delta x} \cdot \frac{(h_{i+\frac{1}{2}}^{+,n} + h_{i-\frac{1}{2}}^{+,n})}{2} + \frac{(z_{i+\frac{1}{2}}^{-,n} - z_{i-\frac{1}{2}}^{-,n})}{\Delta x} \cdot \frac{(h_{i+\frac{1}{2}}^{-,n} + h_{i-\frac{1}{2}}^{-,n})}{2} \right] = \left( h \frac{\partial z}{\partial x} \right)_i \quad (3.19)$$

This manner of discretization allow us to have a scheme which satisfy the conservation property. By inspiration from (3.19), we propose the following decomposition and discretization of the source terms given in Equation (3.1):

$$S_i^n = \frac{1}{2}(S_i^{+,n} + S_i^{-,n}) \text{ and } Q_i^n = \frac{1}{2}(Q_i^{+,n} + Q_i^{-,n}) \quad (3.20)$$

where

$$S_i^{+,n} = \begin{pmatrix} 0 \\ -g \frac{z_{i+\frac{1}{2}}^{+,n} - z_{i-\frac{1}{2}}^{+,n}}{\Delta x} \frac{h_{i+\frac{1}{2}}^{+,n} + h_{i-\frac{1}{2}}^{+,n}}{2} - \frac{(\rho_s - \rho_w)g}{2\rho} \frac{(h_{i+\frac{1}{2}}^{+,n} + h_{i-\frac{1}{2}}^{+,n})^2}{4} \frac{c_{i+\frac{1}{2}}^{+,n} - c_{i-\frac{1}{2}}^{+,n}}{\Delta x} \\ 0 \\ 0 \end{pmatrix}$$

$$S_i^{-,n} = \begin{pmatrix} 0 \\ -g \frac{z_{i+\frac{1}{2}}^{-,n} - z_{i-\frac{1}{2}}^{-,n}}{\Delta x} \frac{h_{i+\frac{1}{2}}^{-,n} + h_{i-\frac{1}{2}}^{-,n}}{2} - \frac{(\rho_s - \rho_w)g}{2\rho} \frac{(h_{i+\frac{1}{2}}^{-,n} + h_{i-\frac{1}{2}}^{-,n})^2}{4} \frac{c_{i+\frac{1}{2}}^{-,n} - c_{i-\frac{1}{2}}^{-,n}}{\Delta x} \\ 0 \\ 0 \end{pmatrix}$$

$$Q_i^{+,n} = \begin{pmatrix} \frac{E^{+,n} - D^{+,n}}{1-p} \\ -g \frac{h_{i+\frac{1}{2}}^{+,n} + h_{i-\frac{1}{2}}^{+,n}}{2} S_f^{+,n} - \frac{(\rho_0 - \rho)}{\rho} \frac{(E^{+,n} - D^{+,n})}{(1-p)} \frac{u_{i+\frac{1}{2}}^{+,n} + u_{i-\frac{1}{2}}^{+,n}}{2} \\ E^{+,n} - D^{+,n} \\ -\frac{E^{+,n} - D^{+,n}}{1-p} \end{pmatrix}$$

and

$$Q_i^{-,n} = \begin{pmatrix} \frac{E^{-,n} - D^{-,n}}{1-p} \\ -g \frac{h_{i+\frac{1}{2}}^{-,n} + h_{i-\frac{1}{2}}^{-,n}}{2} S_f^{-,n} - \frac{(\rho_0 - \rho)}{\rho} \frac{(E^{-,n} - D^{-,n})}{(1-p)} \frac{u_{i+\frac{1}{2}}^{-,n} + u_{i-\frac{1}{2}}^{-,n}}{2} \\ E^{-,n} - D^{-,n} \\ -\frac{E^{-,n} - D^{-,n}}{1-p} \end{pmatrix}$$

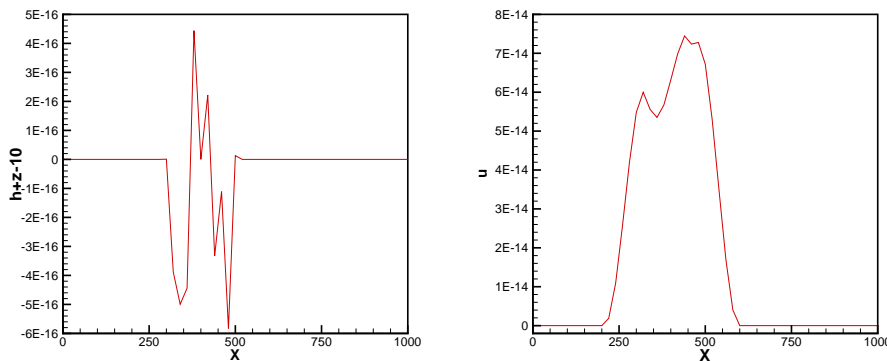


Figure 1:  $h + z - 10$  and  $u$  at  $t = 238000s$  for the modified central upwind scheme.

where  $E^{+,n}$ ,  $D^{+,n}$  and  $S_f^{+,n}$  (respectively  $E^{-,n}$ ,  $D^{-,n}$  and  $S_f^{-,n}$ ) are obtained by replacing  $h$ ,  $u$  and  $c$  by  $\frac{h_{i+\frac{1}{2}}^{+,n} + h_{i-\frac{1}{2}}^{+,n}}{2}$ ,  $\frac{u_{i+\frac{1}{2}}^{+,n} + u_{i-\frac{1}{2}}^{+,n}}{2}$  and  $\frac{c_{i+\frac{1}{2}}^{+,n} + c_{i-\frac{1}{2}}^{+,n}}{2}$  (respectively  $\frac{h_{i+\frac{1}{2}}^{-,n} + h_{i-\frac{1}{2}}^{-,n}}{2}$ ,  $\frac{u_{i+\frac{1}{2}}^{-,n} + u_{i-\frac{1}{2}}^{-,n}}{2}$  and  $\frac{c_{i+\frac{1}{2}}^{-,n} + c_{i-\frac{1}{2}}^{-,n}}{2}$ ) in the expressions of  $E^n$ ,  $D^n$  and  $S_f^n$ .

We will see in the applications below that the modified central upwind scheme proposed in this work capture shocks well with high accuracy and without producing any nonphysical oscillations.

#### 4. Numerical results

In this part of the study, we resolve numerically the coupled model (Equations 2.1-2.2-2.3-2.4) by the proposed modified central upwind scheme (MCUP) with the new discretization of the source term. We present the results for three tests in order to illustrate the capability of the mathematical model and the numerical performance of the schemes with our treatment of the source term.

The first test is made in order to verify the C-property [2,14]. The second one is a dam-break flow over horizontal and frictionless bed in order to assess the accuracy of the numerical model [1,31]. The last test will treat a dam-break flow over mobile bed [2,6,15,16,28,30].

##### 4.1. Verification of the C-property

This test investigates the ability of the modified central upwind scheme to satisfy the exact C-property. The channel length is 1000 m and the initial conditions are defined as:

$$z(x,0) = \begin{cases} \sin^2\left(\frac{(x-300)\pi}{200}\right), & \text{if } 300 \leq x \leq 500 \\ 0, & \text{elsewhere} \end{cases}$$

$$u(x,0) = 0 \text{ m/s}, \quad c(x,0) = 0, \quad h(x,0) = 10 \text{ m} - z(x,0)$$

The discretization uses 50 gridpoints. Table 1 presents the maximum values of  $|h + z - 10|$  and  $u$  at a time  $t = 238000s$  and Figure 1 present the evolution of error  $h + z - 10$  and  $u$  at the same time. We can observe that The free surface profile remains constant during the simulation time which prove that the proposed scheme with the new discretization of the source term satisfy the C-property.

Table 1: Maximum values of  $|h + z - 10|$  and  $u$ .

	$ h + z - 10 $	$u$
MCUP scheme	5.81 E-16	7.52 E-14

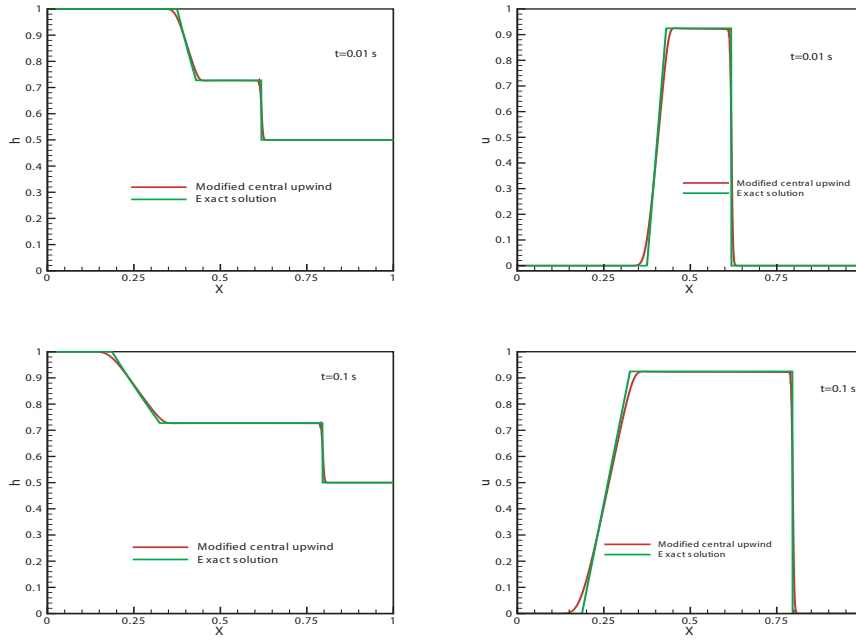


Figure 2: Water free surface and velocity profiles at  $t = 0.04s$  (top) and at  $t = 0.1s$  (bottom).

## 4.2. Performance test

In order to ascertain the convergence of the proposed numerical models, we consider an idealized dam-break flow over a horizontal frictionless and fixed bed, for which the exact solution is known [31]. The domain length is  $L = 1m$  and the initial conditions are given by:

$$h(x) = \begin{cases} 1m, & x \leq 0.5m \\ 0.5m, & x > 0.5m \end{cases} \quad \text{and} \quad u(x, 0) = 0m/s$$

Step size space is  $\Delta x = 5 \times 10^{-3}m$  and  $\Delta t$  is determined according to a specified value of the Courant number  $C_{FL} = 0.85$ . Figure 2 shows the computed and the exact free surfaces and velocity profiles at  $t = 0.04s$  and  $t = 0.1s$ . As can be seen, the obtained solutions approximate very well the exact solutions.

## 4.3. Dam-break over mobile bed

In this subsection, the attention is focused on the behavior of the dam-break flow over a mobile bed [2,30,6,15]. The channel length is 50,000m, the dam is initially located at the middle of the channel  $x = 25,000m$ . The initial conditions are :

$$h(x) = \begin{cases} 40m, & x \leq 25,000m \\ 2m, & x > 25,000m \end{cases}, \quad u(0, x) = 0m/s, \quad c(0, x) = 0.001 \quad (4.1)$$

Initially, the channel bed is considered horizontal and composed of noncohesive uniform sediments. Step size space is  $\Delta x = 10m$  and  $\Delta t$  is computed according to a specified value of  $C_{FL}$  number equal to 0.85.

*4.3.1. Sediments size effect.* In order to show the effect of sediment sizes, we resolve again the coupled model by the the modified central upwind scheme with the proposed discretization in Section 3.4, using different diameters  $d$ .

Figure 3 shows the water free surface and bed profiles with their corresponding concentrations at several times. Figure 4 represents the evolution of the velocity profiles at the same times.

Sediment size acts in different ways according to the type of profile:

- On the water free surface profiles, when the sediment size is great, the jump is more pronounced than that of the small sediment size. The level of water free surface before the abrupt fall remains stable longer when the sediment size is finer. This is in agreement with observations in [15,7,28].
- On the bed change profiles when the sediment size is smaller, the erosion is greater and vice versa, which is logical by the fact that small sediments are easier to be eroded. The same remark has been reported in the simulation of Roe scheme with the new discretization of the source term in [15].
- On the concentration profiles, a heavily concentrated wavefront increases during the initial period (see the concentration profiles at 2min), exceeding 0.5. As expected, more the sediment size is finer, higher concentration is achieved. After this, the wavefront undergoes a lateral expansion (see the concentration profiles at 14min) which is wider when the sediment is fine. This is realistic because the fine particles tend to float while heavy particles tend to fall in the same hydraulic conditions.
- On the velocity profiles the highest value of velocities back to the coarse sediment which is obvious in Figure 4, Also, we note that the wave front reaches a peak velocity (the highest value belongs to the finer sediments), and therefore acquires a strong erosion capacity.

We conclude that the modified central upwind scheme models the dam-break problem by the same way that Roe-scheme proposed in [15].

*4.3.2. Comparison between Roe scheme and Modified central upwind.* Figure 5 describes the evolution of water free surface, bed profiles, the evolution of concentration and velocity profiles at times  $t = 2min$  and  $t = 14min$  by the modified central upwind scheme and Roe scheme proposed in [15] using sediment of diameter  $d = 0.8mm$ .

As can be seen in figure 5, the modified central upwind scheme agree strongly well with Roe scheme developed in [15]. As well as, several observations can be made such as:

- We can observe a hydraulic jump located in the initial position of the dam, then the jump gradually decreases and disappears as it propagates upstream.
- The bed deformation could not be ignored, it has a great influence on the free surface evolution; the bed change must be definitely accounted in the mathematical model (Equations 1-4).
- The eroded sediment amount is closely the same for both schemes.
- The sediment concentration is superimposed except a very teen spade by Roe scheme.
- The velocity is the same for both schemes.

We conclude that the modified central upwind scheme and Roe scheme developed in [15] present the same results and act by the same manner when resolving such physical problem.

## 5. Conclusion

This work deals with the numerical modeling of dam-break flow over an erodible bed. The mathematical model is a combination of the shallow water equations, the transport diffusion equation and the bed morphology change equation. The system is solved by the finite volume central upwind scheme associated with a special treatment of the source term satisfying the conservation property. In order to illustrate the numerical performance of the method, different results of several tests problems are presented. Through the given results, central upwind scheme with the proposed discretization of the source term evinces its performance and capacity by giving accurate results for the water free surface flow and the bed evolution, evenly the effects and interactions on each other. As well, the scheme has given a stable representation of the free surface and bed profiles with a good resolution of the hydraulic jump. The developed modified central upwind scheme agree strongly well with Roe scheme developed in [15] and they present the same results and act by the same manner when resolving the presented physical problem.

## References

1. Ahmad M. F., Mamat M., Wan Nik W. B. and Kartono A., Numerical method for dam break problem by using Godunov approach, *Applied Mathematics and Computational Intelligence*, vol. **2**, pp. 95–107, 2013.
2. Benkhalidoun F., Sari S. and Seaid M., A flux-limiter method for dam-break flows over erodible sediment beds, *Applied Mathematical Modelling*, vol. **36**, pp. 4847–4861, 2012.
3. Bermudez A., Vazquez M., Upwind methods for Hyperbolic Conservation Laws with Source Terms, *Computers and Fluids*, vol. **23**, pp.1049–1071, 1994.
4. Cao Z. and Carling P. A., Mathematical modelling of alluvial rivers: reality and myth: Part II, *Proceedings of the Institution of Civil Engineers - Water and Maritime*, vol. **154(4)**, pp. 297–307, 2002.
5. Cao Z., Day R. and Egashira S., Coupled and decoupled numerical modelling of flow and morphological evolution in alluvial rivers, *Journal of Hydraulic Engineering*, vol. **128**, pp. 306–321, 2002.
6. Cao Z., Pender G., Wallis S. and Carling P. A., Computational dam-break hydraulics over erodible sediment bed, *Journal of Hydraulic Engineering*, **130**, pp. 389–703, 2004.
7. Capart H. and Young D. L., Formation of a jum by the dam-break wave over a granular bed, *Journal of Fluid Mechanics*, **372**, pp. 165–187, 1998.
8. Chertock A., Cui S., Kurganov A., Wu T., Well-balanced positivity preserving central-upwind scheme for the shallow water system with friction terms, *International Journal for numerical methods in Fluids*, **78**, pp. 355–383, 2015.
9. Ferreira R. and Leal J., 1D mathematical modeling of the instantaneous dam-break flood wave over mobile bed: application of TVD and flux-splitting schemes, *Proceedings of European Concerted Action on Dam-break Modeling*, Munich, Germany, pp. 175–222, 1998.
10. Fraccarollo L. and Capart H., Riemann wave description of erosional dam-break flows. *Journal of Fluid Mechanics*, vol. **461**, pp. 183–228, 2002.
11. Fraccarollo L. and Armanini A., A semi-analytical solution for the dam-break problem over a movable bed, *Proceedings of European Concerted Action on Dam-Break Modeling*, Munich, Germany, pp. 145–152, 1998.
12. Gottlieb S. and Chi-Wang S., Total variation diminishing Runge-Kutta schemes, *Mathematics of computation*, vol. **67**, pp. 73–85, 1998.
13. He S., Liu W., Li X., Ouyang C., An improved coupling model for water flow, sediment transport and bed evolution, *Geoscientific Model Development Discussions*, vol. **7**, pp. 2429–2457, 2014.
14. Hudson J. and Sweby P. K., Formulations for numerically approximating hyperbolic systems governing sediment transport, *Journal of Scientific Computing*, vol. **19**, pp. 225–252, 2003.
15. S. Jelti, M. Mezouari, M. Boulerhcha, Numerical modeling of dam-break flow over erodible bed by Roe scheme with an original discretization of source term, *International Journal of Fluid Mechanics Research*, Vol. **45** (1), pp. 21–36, 2018.
16. S. Jelti and M. Boulerhcha, Numerical modeling of two dimensional non-capacity model for sediment transport by an unstructured finite volume method with a new discretization of the source term, *Mathematics and Computers in Simulation*, Vol. **197**, pp. 253–276, 2022.
17. S. Jelti, A. Charhabil and J. El Ghordaf, Numerical Modeling of Non-capacity Model for Sediment Transport by Central Upwind Scheme, *Journal of Applied Mathematics and Informatics*, Vol. **41** (1), pp. 181–192, 2023.
18. Hosseinzadeh-Tabrizi A., Ghaeini-Hessaroeiyeh M., Coupled dam-break flow and bed load modelling using HLLC-WAF scheme, *Water Sci. Technol.*, 72(7), 1155–1167, 2015.
19. Kesserwani G., Shamkhalchian A. and Zadeh M. J., Fully coupled discontinuous galerkin modeling of dam-break flows over movable bed with sediment transport, *Journal of Hydraulic Engineering, Technical Notes*, vol. **140(4)**, DOI: 10.1061/(ASCE)HY.1943-7900.0000860, 2014.
20. Kurganov A, Tadmor E. New high resolution central schemes for nonlinear conservation laws and convection-diffusion equations. *J. Comput. Phys.* 160 (2000) 241-282.
21. Kurganov A, Noelle S, Petrova G. Semi-discrete central-upwind scheme for hyperbolic conservation laws and Hamilton-Jacobi equations. *SIAM Journal on Scientific Computing* 23 (2001), 707–740.
22. Kurganov A, Levy D. Central-upwind schemes for the saint-venant system. *ESAIM: Mathematical Modelling and Numerical Analysis* 36 (2002),397–425.
23. Kurganov A, Petrova G. A second-order well-balanced positivity preserving central-upwind scheme for the saintvenant system. *Communications in Mathematical Sciences* 5 (2007), 133–160.
24. Kurganov A, Lin C-T. On the reduction of numerical dissipation in central-upwind schemes. *Communications in Computational Physics* 2(1) (2007),141-163.
25. Kurganov A, Tadmor E. Solution of two-dimensional Riemann problems for gas dynamics without Riemann problem solvers. *Numerical Methods for Partial Differential Equations* 18 (5) (2002); 584-608.

26. Kurganov A, Petrova G. Central-upwind schemes for two-layer shallow equations. *SIAM Journal on Scientific Computing* 31 (3) (2009),1742-1773.
27. LeVeque R. J., *Finite Volume Methods for Hyperbolic Problems*, Cambridge: Cambridge University Press, 2002.
28. Li S. and Duffy C. J., Fully coupled approach to modeling shallow water flow, sediment transport and bed evolution in rivers, *Water Resources Research*, vol. **47**, pp. 1–20, 2011.
29. Roe P. L., Approximate Riemann solvers, parameter vectors and difference schemes, *Journal of Computational Physics*, vol. **43**, pp. 357–372, 1981.
30. Simpson G. and Castelltort S., Coupled model of surface water flow, sediment transport and morphological evolution, *Computers and geosciences*, vol. **32**, pp. 1600–1614, 2006.
31. Stoker J. J., *Water Waves, The Mathematical Theory and Applications*, New York: Wiley-Interscience Publication, 1992.
32. Van Rijn L. C., Sediment transport, part II: suspended load transport, *Journal of Scientific Computing*, vol. **110**, pp. 1613–1641, 1984.
33. Wu W., *Computational River Dynamics*, London: Taylor and Francis, 2008.
34. Wu W. and Wang S. S., One-dimensional modeling of dam-break flow over movable beds, *Journal of Hydraulic Engineering*, vol. **133**, pp. 48–58, 2007.
35. Yang C. T. and Greimann B. P., Dam-break unsteady flow and sediment transport, *Proceedings of European Concerted Action on Dam-Break Modeling*, Zaragoza, Spain, pp. 327–365, 1999.
36. Yue Z., Liu H., Li Y., Hu P. and Zhang Y., A Well-Balanced and Fully Coupled Noncapacity Model for Dam-Break Flooding, *Mathematical Problems in Engineering*, vol. **2015**, Article ID 613853, 13 pages, 2015.

S. Jelti,  
M/E Laboratory, FSO,  
Mohammed First University,  
60050 Oujda, Morocco.  
E-mail address: s.jelti@ump.ac.ma

and

A. Serghini,  
ANNA reasearch team, LANO Laboratory, FSO-ESTO,  
Mohammed First University,  
60050 Oujda, Morocco.  
E-mail address: a.serghini@ump.ac.ma

and

A. El Hajaji,  
LIRO Laboratory, ENCGJ, Chouaib Doukkali University  
Eljadida, Morocco.  
E-mail address: a\_elhajaji@yahoo.fr

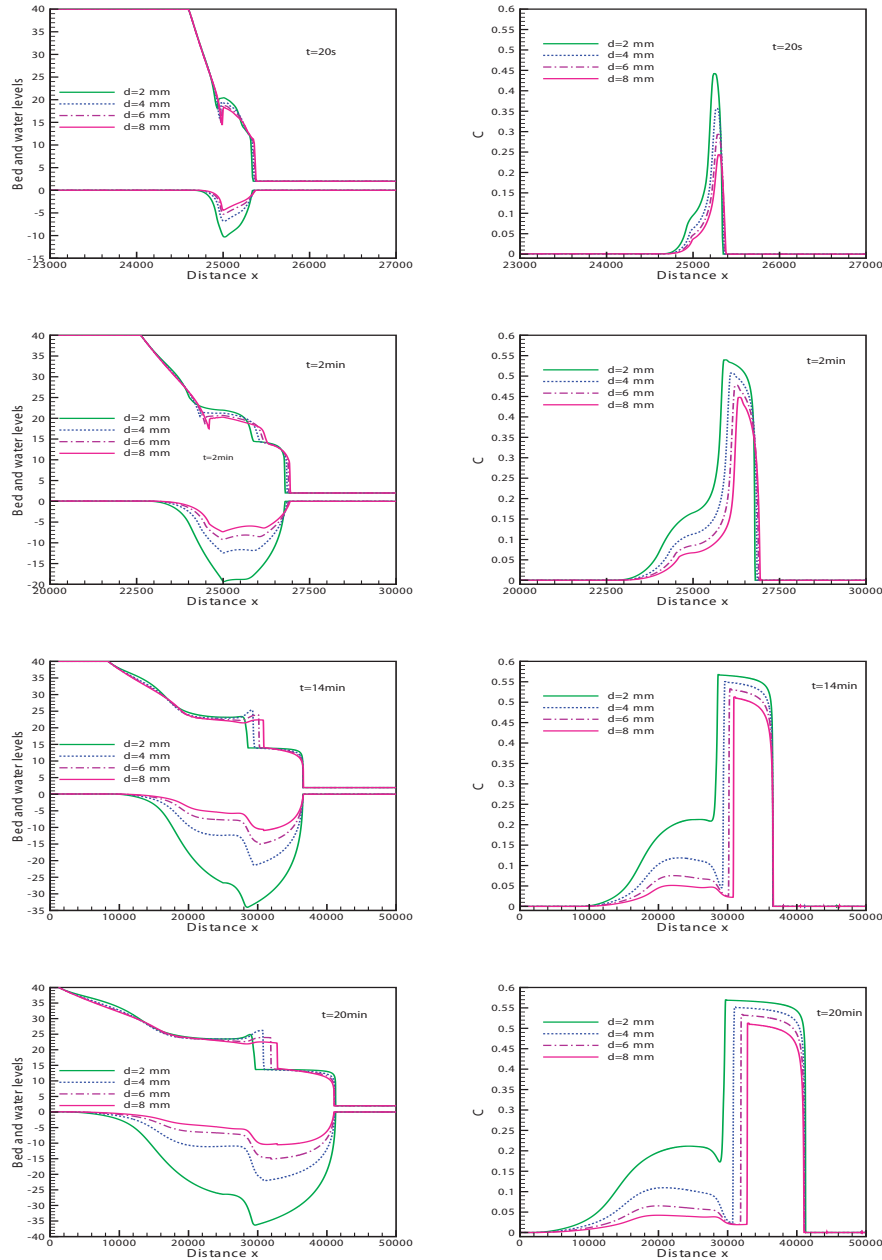


Figure 3: Water free surface and bed profiles with their corresponding concentrations for different sizes of sediment.

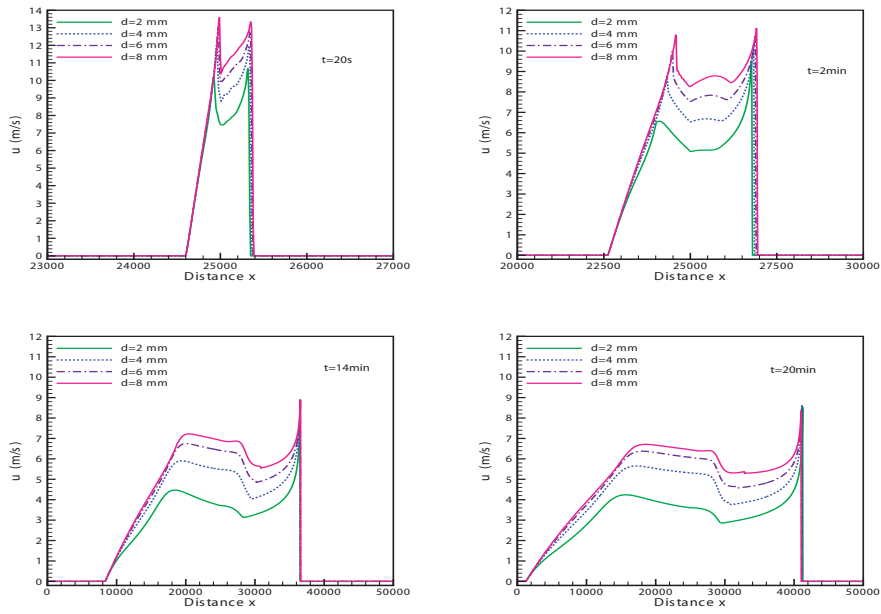


Figure 4: Velocity profiles at different times for different sizes of sediment.

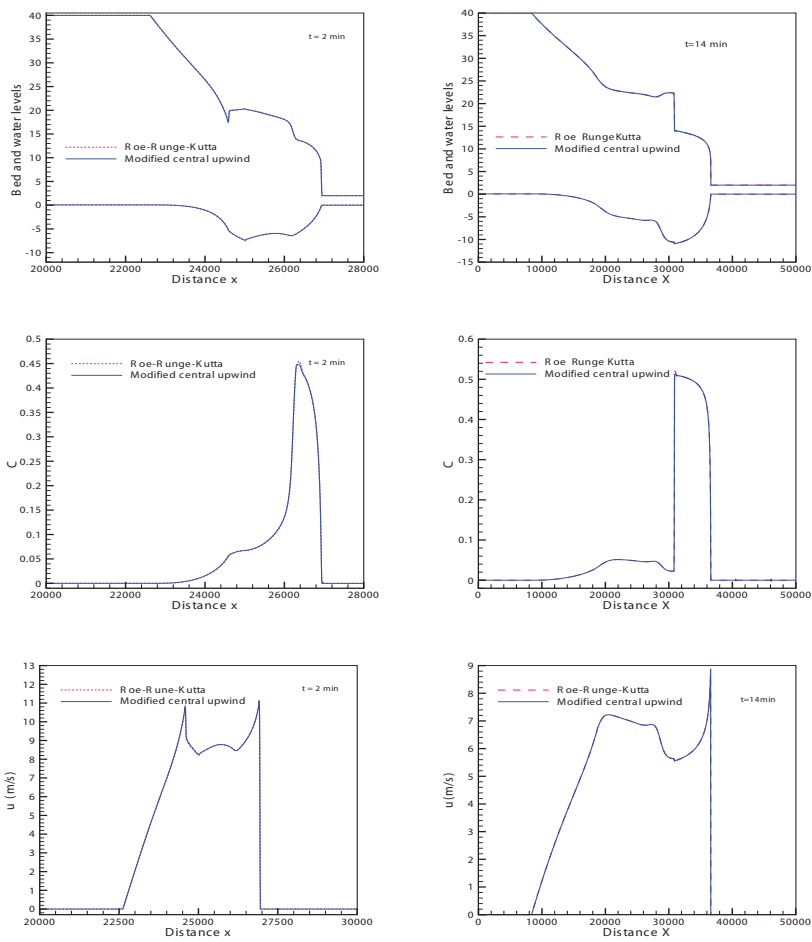


Figure 5: Comparison of Modified central upwind and Roe scheme of Water free surface, bed profiles, concentration and velocity at  $t = 2\text{min}$  and  $t = 14\text{min}$  for  $d = 8\text{mm}$ .